AMERICAN SOCIETY FOR MICROBIOLOGY | Infection and Immunity

The Metalloprotease Mpl Supports *Listeria monocytogenes* Dissemination through Resolution of Membrane Protrusions into Vacuoles

Diego E. Alvarez,[a] Hervé Agaisse[b]

Instituto de Investigaciones Biotecnológicas, CONICET, Universidad Nacional de San Martín, San Martín, Argentina[a]; Department of Microbiology, Immunology, and Cancer Biology, University of Virginia School of Medicine, Charlottesville, Virginia, USA[b]

Listeria monocytogenes **is an intracellular pathogen that disseminates within the intestinal epithelium through acquisition of actin-based motility and formation of plasma membrane protrusions that project into adjacent cells. The resolution of membrane protrusions into vacuoles from which the pathogen escapes results in bacterial spread from cell to cell. This dissemination process relies on the *mlp-actA-plcB* operon, which encodes ActA, a bacterial nucleation-promoting factor that mediates actin-based motility, and PlcB, a phospholipase that mediates vacuole escape. Here we investigated the role of the metalloprotease Mpl in the dissemination process. In agreement with previous findings showing that Mpl is required for PlcB activation, infection of epithelial cells with the Δ*plcB* or Δ*mpl* strains resulted in the formation of small infection foci. As expected, the Δ*plcB* strain displayed a strong defect in vacuole escape. However, the Δ*mpl* strain showed an unexpected defect in the resolution of protrusions into vacuoles, in addition to the expected but mild defect in vacuole escape. The Δ*mpl* strain displayed increased levels of ActA on the bacterial surface in protrusions. We mapped an Mpl-dependent processing site in ActA between amino acid residues 207 to 238. Similar to the Δ*mpl* strain, the Δ$actA_{207–238}$ strain displayed increased levels of ActA on the bacterial surface in protrusions. Although the Δ$actA_{207–238}$ strain displayed wild-type actin-based motility, it formed small infection foci and failed to resolve protrusions into vacuoles. We propose that, in addition to its role in PlcB processing and vacuole escape, the metalloprotease Mpl is required for ActA processing and protrusion resolution.**

Intracellular pathogens such as *Listeria monocytogenes*, *Shigella flexneri*, or *Rickettsia* spp. hijack the host actin assembly machinery to acquire actin-based motility in the cytosol of an infected cell and spread from cell to cell (1). Motile bacteria in a primary infected cell extend membrane protrusions that are resolved into double-membrane vacuoles from which bacteria escape to initiate a new replication cycle in adjacent cells (2–5).

Listeria monocytogenes actin-based motility requires the expression of the bacterial nucleation-promoting factor ActA (6–8), which recruits and activates the host cell actin nucleator, the ARP2/3 complex (9, 10). ActA is coexpressed as an operon of three genes encoding the metalloprotease Mpl, ActA itself, and the phospholipase PlcB (11). The expression of the operon is driven by two promoters located upstream of Mpl and ActA (12, 13). The transcriptional regulator PrfA activates both promoters as the bacteria reach the host cell cytosol (14). ActA is secreted at distinct sites along the sides of bacteria and anchored to the peptidoglycan (15). Upon bacterial growth and division, cell wall dynamics leads to accumulation of ActA at the bacterial pole (15, 16). ActA polarization results in ARP2/3-dependent actin assembly at the bacterial pole, which propels the bacteria throughout the cytosol of infected cells.

Several bacterial factors have been implicated in vacuole escape, including the phosphatidylinositol-specific phospholipase C (PlcA) (17), the broad-range phospholipase C (PlcB) (18), and the metalloprotease (Mpl) (16). Both PlcB and Mpl are synthesized as inactive proenzymes that accumulate at the membrane-cell wall interface (19–22). A decrease in pH initiates Mpl autoactivation through self-cleavage, leading to the maturation of PlcB through Mpl-mediated cleavage of the N-terminal propeptide of PlcB (23, 24). Mpl autoactivation also leads to the rapid secretion of Mpl and PlcB across the cell wall into the vacuolar space, where PlcB challenges the integrity of the vacuole membrane by hydrolyzing membrane phospholipids (25).

In contrast to our knowledge of the mechanisms supporting actin-based motility and vacuole escape, our understanding of the mechanisms supporting protrusion resolution is limited. As motile bacteria encounter the plasma membrane, they form membrane protrusions that elongate for a short time and then display fitful movement until resolution into vacuoles occurs (2). Recent studies have revealed cellular factors supporting the resolution process, including the casein kinase CSNK1 (26) and cytoskeleton factors such as the ARP2/3 complex and components of the actin network disassembly machinery (27). A model of *L. monocytogenes* protrusion resolution in which the activity of the actin network disassembly machinery is critical for exhausting the actin network from the distal region in pro-

Received 12 February 2016 **Returned for modification** 4 March 2016
Accepted 1 April 2016

Accepted manuscript posted online 11 April 2016

Citation Alvarez DE, Agaisse H. 2016. The metalloprotease Mpl supports *Listeria monocytogenes* dissemination through resolution of membrane protrusions into vacuoles. Infect Immun 84:1806–1814. doi:10.1128/IAI.00130-16.

Editor: C. R. Roy, Yale University School of Medicine

Address correspondence to Hervé Agaisse, hfa5y@virginia.edu.

Supplemental material for this article may be found at http://dx.doi.org/10.1128/IAI.00130-16.

trusions was recently proposed (27). The disassembled network fuels the continuous activity of the assembly machinery at the bacterial pole. Efficient actin assembly in nonelongating protrusions generates tension forces that challenge the plasma membrane and contribute to vacuole formation. Besides ActA and its role in actin polymerization, it is unclear whether additional bacterial factors may contribute to the resolution of protrusions into vacuoles. Here, we demonstrate a role for the metalloprotease Mpl not only in PlcB processing and vacuole escape but also in ActA processing and resolution of protrusions into vacuoles.

MATERIALS AND METHODS

Bacterial and mammalian cell growth conditions. *Listeria monocytogenes* strain 10403S (28) harboring plasmid pHT315-hspk (a derivative of plasmid pHT315 conferring erythromycin resistance [29]) and encoding green fluorescent protein (GFP) under the control of the IPTG (isopropyl-β-D-thiogalactopyranoside)-inducible *Phyperspank* promoter (a gift from D. Rudner) was grown overnight in brain heart infusion (BHI; Difco) supplemented with 10 μg/ml erythromycin (Gibco) at 30°C without agitation prior to infection. HeLa 229 (ATCC CCL-2.1) cells were grown in high-glucose Dulbecco's modified Eagle's medium (DMEM; Invitrogen) supplemented with 10% fetal bovine serum (FBS; Gibco) at 37°C in a 5% CO_2 incubator.

Generation of recombinant *L. monocytogenes* strains. All primers, plasmids, and strains used in this study are listed in the tables in the supplemental material. A PCR fragment spanning the *mpl-actA-plcB* operon was cloned into pHT304 vector (29) between the EcoRI and BamHI sites. In-frame deletion of *mpl* was generated by partial digestion of p304*mpl-actA-plcB* with HindIII and religation. p304 Δ$mpl_{48–503}$-*actA-plcB* was digested with SphI and, after 5′ overhang fill-in, with EcoRI to excise a 1.4-kb fragment that was cloned into pMAD vector (30) between EcoRI and SmaI. The resulting plasmid, pMAD Δ$mpl_{48–503}$, was introduced into *L. monocytogenes* strain 10403S by electroporation, and the allele replacement was conducted as previously described (30). *L. monocytogenes* mutant strain 10403S Δ$mpl_{48–503}$ was verified by PCR amplification using chromosomal DNA of the corresponding strain and direct DNA sequencing of the PCR product.

A triple Flag sequence was introduced in ActA by overlapping PCR using flanking primers ActAEco and ActA3BamHI, and overlapping primers 3×Fsense and 3×Fantisense containing the 3×Flag sequence. The PCR product was digested with EcoRI and BamHI and cloned into pMAD. The resulting plasmid, pMAD-3xFlagActA, was used for allele replacement in *L. monocytogenes* 10403S or 10403S Δ$mpl_{48–503}$ to generate strains 10403S 3×Flag-*actA* and 10403S Δ$mpl_{48–503}$ 3×Flag-*actA*, respectively.

Triple Flag-ActA sequence from pMAD-3xFlagActA was subcloned into p304*mpl-actA-plcB* between HpaI and KpnI. To delete amino acid residues 207 to 238 in ActA, first the PCR product amplified using primers Δ207-38 sense and actA3BamHI was cloned into p304*mpl-3xFactA-plcB* between ClaI and KpnI. Then, a fragment encompassing the *actA* deletion was excised by digestion of p304*mpl-3xF actA*Δ$_{207–238}$-*plcB* with HpaI and StuI and subcloned into a unique SmaI site in pMAD. The resulting plasmid, pMAD-3xFlag *actA*Δ$_{207–238}$, was used for allele replacement in *L. monocytogenes* 10403S to generate strain 10403S 3×Flag-*actA*Δ$_{207–238}$.

Complementation of *L. monocytogenes*. A PCR fragment carrying the *mpl* promoter and open reading frame (ORF) sequences followed by the *plcB* terminator was amplified with primers pMplEco and mpl HPB-glII antisense and cloned between the EcoRI and BamHI sites in pHT-304 to give p304*mpl*. *L. monocytogenes* 10403S Δ$mpl_{48–503}$ was electroporated with p304*mpl* plasmid, and transformants were selected on BHI agar supplemented with erythromycin (10 μg/ml).

***L. monocytogenes* infection, imaging, and image analysis.** On day 0, HeLa 229 cells were seeded on coverslips. On day 1, cells were transfected with the pDsRed-Monomer-Membrane DNA construct (Clontech) encoding DsRed-Monomer fused to the N-terminal 20 amino acids of neuromodulin, which target the fluorescent protein to the plasma membrane. The medium was replaced on day 2, and confluent monolayers of cells were infected at a multiplicity of infection (MOI) of 10 with *L. monocytogenes* by centrifugation at 200 × *g* for 5 min. After 1 h of incubation at 37°C, noninternalized bacteria were killed with gentamicin (final concentration, 50 μg/ml). Six hours postinfection, cells were washed three times with phosphate-buffered saline (PBS) and fixed in PBS–4% paraformaldehyde. Coverslips were processed for imaging and mounted onto glass slides using Dabco antifade mounting medium. Low-magnification images were acquired on a Nikon TE2000 microscope with a 10× objective, and image analysis was conducted using the MetaMorph software as described in Fig. S1 in the supplemental material. High-magnification images were acquired on a Nikon TE2000 spinning disc confocal microscope with a 60× oil objective (numerical aperture [NA], 1.4) and processed using the Volocity software package (Improvision/PerkinElmer).

Numeration of membrane protrusions and vacuoles. For membrane protrusion and vacuole formation quantifications, GFP expression of internalized bacteria was induced by IPTG (10 mM final). The proportion of bacteria found in protrusions or vacuoles or free in neighboring cells was assessed after accumulating a total of no fewer than 500 bacteria in three independent experiments (26).

Quantification of the levels of ActA expression on the bacterial surface. For quantifications of surface levels of ActA, fixed cells were immunostained with mouse M2 monoclonal antibody anti-FLAG (1:1,000) obtained from Sigma followed by Alexa Fluor secondary antibody (1:1,000). ActA levels on the surface of bacteria in protrusions were quantified on three-dimensional (3D) reconstructions of the confocal images using the line profile measurement module of the Volocity software. The ActA levels represent the mean absolute intensity value in the FLAG channel obtained from a line drawn along bacteria. The front pole of bacteria was defined by a 2-fold increase of intensity above background levels in the pDsRed-Monomer-Mem channel. The intensity value in the FLAG channel at the front pole of bacteria was used as the lower limit to define the rear pole of bacteria. Surface levels of ActA were assessed for at least 50 bacteria.

Western blotting. Cells infected with *L. monocytogenes* for 8 h were washed once with 1× PBS and lysed for 30 min in 300 μl of lysis buffer (20 mM Tris [pH 7.5], 150 mM NaCl, 2 mM EDTA, 1% Triton X-100, 1 mM phenylmethylsulfonyl fluoride [PMSF], and protease inhibitor cocktail [Roche]). The lysates were centrifuged at 13,000 rpm for 10 min. The clarified lysates were incubated overnight at 4°C in the presence of 10 μl of anti-FLAG M2 agarose beads (Sigma). The beads were washed 3 times (20 mM Tris [pH 7.5], 150 mM NaCl, 2 mM EDTA, 1% Triton X-100), and the pellet was resuspended in 2× Laemmli sample buffer. Protein samples were separated by SDS-PAGE and analyzed by immunoblotting using mouse M2 monoclonal antibody anti-FLAG followed by horseradish peroxidase (HRP)-conjugated secondary antibody and Amersham ECL Western blotting detection reagents.

Cytosolic motility. Cells seeded on 35-mm imaging dishes (MatTek, Ashland, MA) were transfected with the pDsRed-Monomer-Membrane DNA construct (Clontech) the day before infection with GFP-expressing *L. monocytogenes*. Cells expressing pDsRed-Monomer-Membrane were imaged between 3 and 5 h postinfection. Images were captured every 15 s for 10 min on a Nikon TE2000E spinning disc confocal microscope. Single-bacterium tracking was performed using the tracking module of the Volocity software (Improvision, Lexington, MA). Velocity was recorded for at least 40 bacteria per strain.

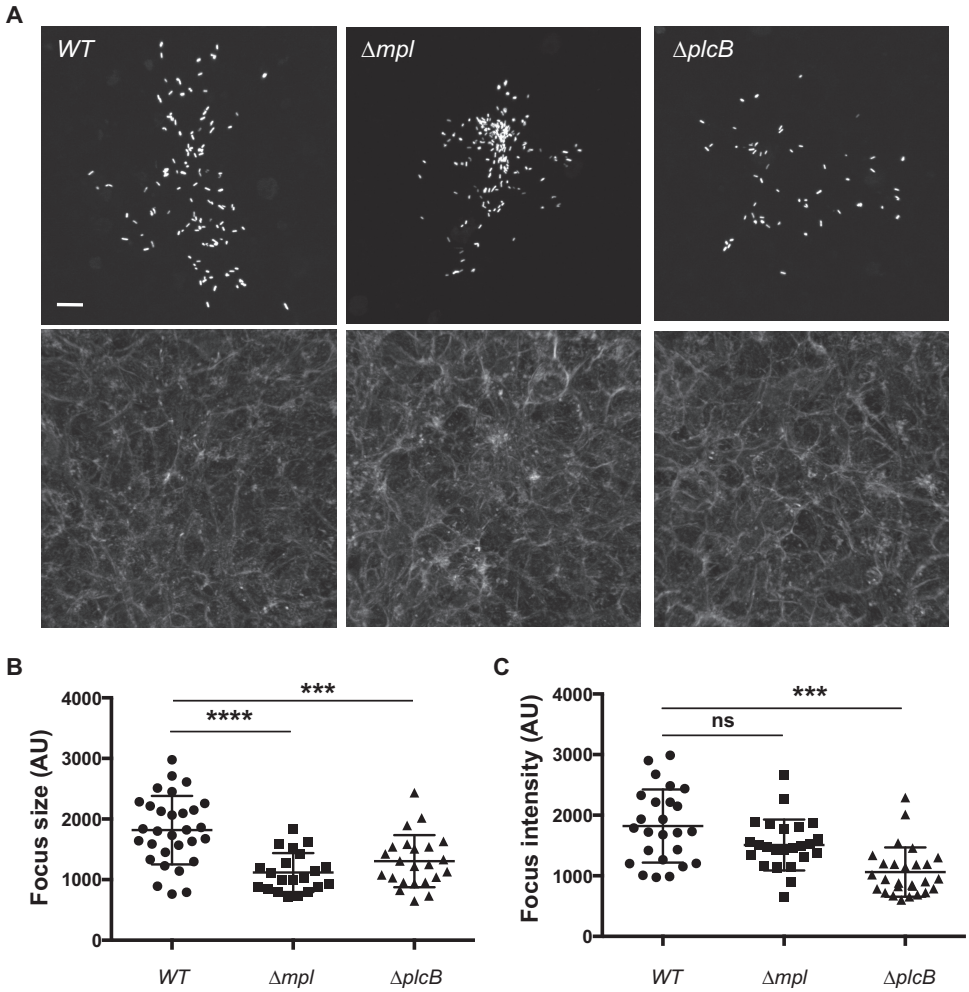

FIG 1 Characterization of the infection foci formed in cells infected with the wild type (WT) or the *mpl* or *plcB* mutant. (A) Representative images showing monolayers of confluent HeLa 229 cells infected with GFP-expressing *L. monocytogenes* for 6 h (top, GFP-expressing bacteria; bottom, phalloidin staining). Bar, 10 μm. (B) Sizes of the infection foci (AU, arbitrary units) as determined by computer-assisted analysis of images like those shown in panel A. One-way analysis of variance (ANOVA) with Tukey's posttest: Δ*mpl* versus WT strain, $P < 0.0001$ (****); Δ*plcB* versus WT strain, $P < 0.001$ (***). (C) Average GFP intensity per infection focus as determined by computer-assisted analysis of images shown in panel A. One-way ANOVA with Tukey's posttest: Δ*mpl* versus WT strain, not significant (ns); Δ*plcB* versus WT strain, $P < 0.001$ (***).

RESULTS

Mpl and PlcB are required for the formation of WT infection foci. As determined by standard plaque formation assays (31), the metalloprotease Mpl and the phospholipase PlcB are required for *L. monocytogenes* spread from cell to cell (32). To further investigate the spreading defects displayed by the *mpl* and *plcB* mutants, we used fluorescence microscopy to compare the sizes of the infection foci formed by *L. monocytogenes* in confluent epithelial cells 8 h after invasion (26, 27) (Fig. 1A). As expected, given the role of PlcB in vacuole escape and given the role of Mpl in PlcB processing and activation (11, 20, 33), both mutants formed infection foci that were small compared to those of wild-type (WT) bacteria (Fig. 1A). We quantified these observations by computer-assisted image analysis (see Fig. S1 in the supplemental material), demonstrating 39% ($P < 0.0001$) and 27% ($P < 0.001$) decreases in the size of the foci formed in cells infected with the *mpl* and *plcB* mutants, respectively (Fig. 1B). Interestingly, we noticed striking differences in the scattering of the bacteria within the formed infection foci. Whereas the *plcB* mutant displayed an evenly scattered distribution in a given infection focus, similar to the foci formed by wild-type bacteria (Fig. 1A, WT and *plcB*), the *mpl* mutant seemed to accumulate in the center of the infection foci, presumably in the primary infected cells (Fig. 1A, *mpl*). Previously, we encountered two situations that led to accumulation of bacteria in primary infected cells: (i) bacteria displaying defects in actin-based motility (27, 34) and (ii) bacteria displaying wild-type actin-based motility but forming protrusions that failed to resolve into vacuoles and ultimately collapsed, bringing the bacteria back to the primary infected cells (26, 27). To examine the former possibility, we tracked the *mpl* mutant in the cytosol of infected cells. The intracellular motility of the *mpl* mutant was indistinguishable from that of the wild type (see Fig. S2 in the supplemental material). Altogether, these results confirm the involvement of the metalloprotease Mpl in *L. monocytogenes* spread from cell to cell and reveal a potential role for Mpl in the resolution of protrusions into vacuoles.

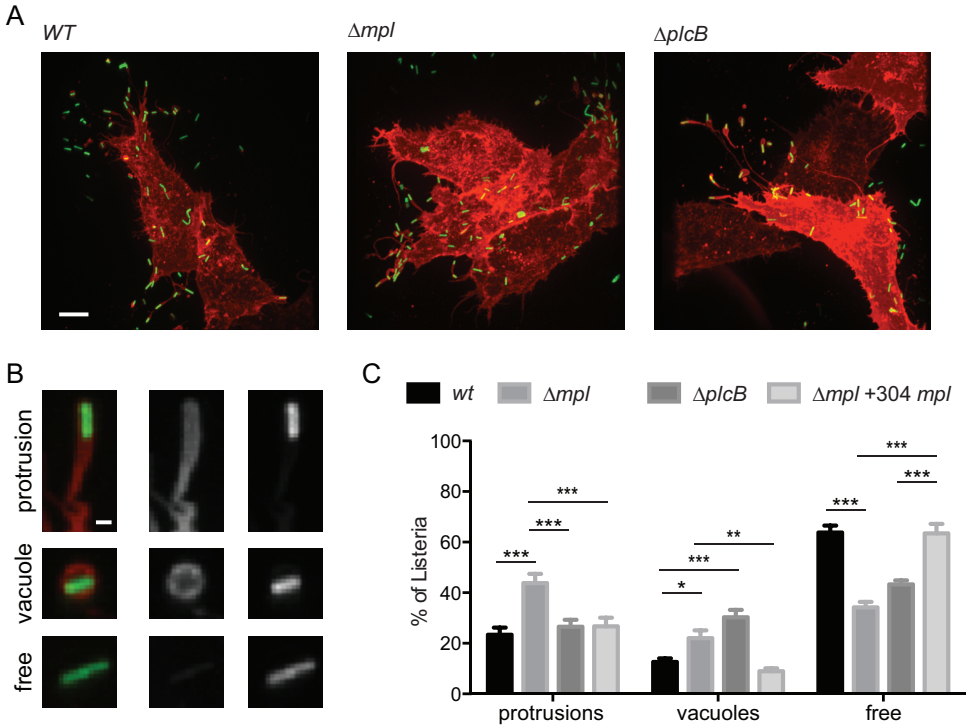

FIG 2 Protrusion resolution and vacuole escape in cells infected with the *mpl* and *plcB* mutants. (A) Representative images showing HeLa 229 cells transiently transfected with the plasma membrane-targeted dsRed constructs and infected with GFP-expressing *L. monocytogenes* for 6 h (green, bacteria; red, membrane). Bar, 10 μm. (B) Representative images of spreading bacteria in protrusions (top panel), in double-membrane vacuoles (middle panel), and not associated with membrane marker (bottom panel). Left, merged image (green, bacteria; red, plasma membrane). Middle, plasma membrane only. Right, bacteria. Bar, 1 μm. (C) Percentages of spreading bacteria in protrusions, in vacuoles, and free in adjacent cells in cells infected with wild-type bacteria or *mpl* or *plcB* mutants. Data are presented as means and standard deviations for three independent samples and were analyzed by two-way ANOVA with Tukey's posttest using PRISM 5 (GraphPad Software). ***, $P < 0.001$; **, $P < 0.01$; *, $P < 0.05$.

Role of Mpl in the resolution of protrusions into vacuoles. To further investigate the potential role of Mpl in protrusion resolution, we used a fluorescence microscopy-based assay allowing for the visualization of the plasma membrane of primary infected cells and the numeration of bacteria that already crossed the boundary of primary infected cells (spreading bacteria) located in membrane protrusions or vacuoles and bacteria no longer associated with the membrane marker and therefore free in the cytosol of adjacent cells (Fig. 2A and B) (26, 27). Our previous work showed that the formation of protrusions that do not resolve into vacuoles correlates with an increase in the numbers of bacteria found in protrusions (26, 27). In cells infected with wild-type bacteria, less than 25% of the spreading bacteria were found in protrusions (Fig. 2C). This was in contrast with the situation observed in cells infected with the *mpl* mutant, in which more than 45% of the spreading bacteria were found in protrusions (Fig. 2C). In order to demonstrate the specificity of the observed phenotype, we transformed the *mpl* strain with a low-copy-number plasmid harboring the full-length *mpl* gene expressed from its own promoter (yielding the *mpl*;*p304mpl* strain). The numbers of protrusions formed in cells infected with the *mpl*;*p304mpl* strain were similar to the numbers scored in cells infected with wild-type bacteria, indicating a complete rescue of the phenotype observed in cells infected with the *mpl* mutant (Fig. 2C). In contrast to the results obtained in cells infected with the *mpl* mutant, we did not observe any significant differences between the numbers of protrusions scored in cells infected with wild-type bacteria or the *plcB* mutant (Fig. 2C), suggesting that the activity of PlcB is not required for efficient resolution of protrusions into vacuoles. Altogether, these results establish that, independent of its role in PlcB activation, Mpl is required for the resolution of protrusions into vacuoles.

PlcB and Mpl are required for vacuole escape. In addition to membrane protrusions, we also characterized the numbers of vacuoles present in cells infected with the *plcB* or the *mpl* mutant. Compared to wild-type bacteria, we observed a 3-fold increase in the number of bacteria trapped in vacuoles in cells infected with the *plcB* mutant (Fig. 2C), reflecting the previously described role for PlcB in vacuole escape. We also noticed that the total GFP signal per infection focus, which is proportional to the number of bacteria present in a given infection focus, was significantly lower in cells infected with the *plcB* mutants (Fig. 1C). This presumably reflected the fact that bacteria trapped into vacuoles do not grow/divide as fast as bacteria that successfully escaped vacuoles and resided in the cytosol. Similar to what was seen with the *plcB* mutant, we also observed a significant increase in the number of vacuoles in cells infected with the *mpl* mutant, although the phenotype was not as striking as the one observed with the *plcB* mutant (Fig. 2C). In agreement with the milder vacuole escape defect observed with the *mpl* mutant, the GFP signal per infection focus was lower than, but not statistically different from, that of the wild type (Fig. 1C). These results demonstrate that, in agreement with the established role of Mpl in the proteolytic activation of PlcB, Mpl is required for vacuole escape, although

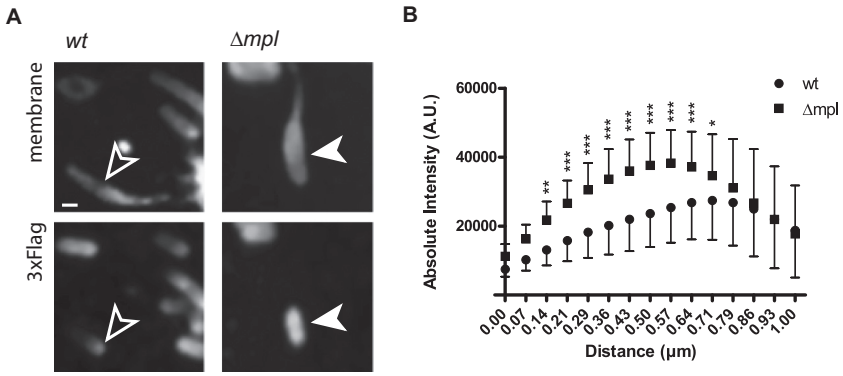

FIG 3 Distribution of ActA on the surface of wild-type and Δ*mpl* mutant bacteria forming protrusions. (A) Representative images showing the distribution of 3×Flag-ActA on the surface of bacteria in protrusions. Top panels, plasma membrane. Bottom panels, FLAG staining. Bar, 1 μm. (B) Quantitative analysis of ActA distribution on the bacterial surface. The absolute intensity of the fluorescence signal in the FLAG channel is represented against the normalized distance from the front pole. Data are represented as means and standard deviations and were analyzed by two-way ANOVA using PRISM 5 (GraphPad Software). ***, $P < 0.001$; **, $P < 0.01$; *, $P < 0.05$.

the main observed defect is a failure to resolve protrusions into vacuoles (Fig. 2C).

Mpl regulates ActA polarization in protrusions. To further understand the role of Mpl in protrusion resolution, we explored the possibility that Mpl-dependent processing of ActA may regulate the levels of ActA on the bacterial surface in protrusions. This hypothesis stemmed from the facts that (i) ActA was previously shown to be subject to Mpl-dependent degradation, although degradation was proposed to occur in vacuoles (2), (ii) ActA polarization is central to efficient actin polymerization in the cytosol (15, 16, 35), and (iii) efficient actin polymerization is essential for the resolution of protrusions into vacuoles (27). To investigate ActA polarization, we generated a version of ActA tagged with a 3×Flag epitope inserted between the AVC domain (encompassing the *a*cidic stretch, *v*erprolin homology, and *c*entral region) and the proline-rich region (PRR) of ActA, referred to as ActA-3xF. The infectivity and the ability of the ActA-3xF-expressing strain to spread from cell to cell were indistinguishable from those of the wild type (see Fig. S3 in the supplemental material). The intensity of the Flag signal was quantified along the bacterial length for wild-type bacteria and the *mpl* mutant located in protrusions. We observed a polarized distribution of the signal on wild-type bacteria, with high levels of ActA expression at the bacterial pole (Fig. 3A and B; see also Fig. S4 in the supplemental material). In contrast, the *mpl* mutant showed a striking increase in the levels of the Flag signal along the bacterial side (Fig. 3A and B; see also Fig. S4 in the supplemental material). Altogether, these results suggest that Mpl contributes to ActA polarization by regulating the levels of ActA expression on the bacterial surface.

Mapping of an Mpl-dependent processing site in ActA. As the surface levels of ActA were significantly higher in the protrusions formed in cells infected with the *mpl* mutant, we next attempted to locate a putative Mpl-dependent processing site in ActA. To this end, cells infected with bacteria expressing ActA-3xF were lysed and ActA-3xF was immunoprecipitated and analyzed by Western blotting. For wild-type bacteria, we detected peptides in the ~90-kDa range, corresponding to full-length ActA bearing posttranslational modifications, as previously reported (7). Interestingly, we also detected an ~30-kDa peptide, which was not detected in the samples extracted from cells infected with the *mpl* mutant (Fig. 4A). Given the position of the 3× Flag epitope in ActA-3xF (Fig. 4B), and given the fact that the 30-kDa peptide was also observed when the 3×Flag epitope was introduced between the A and V regions of the AVC domain (data not shown), we hypothesized that the 30-kDa peptide resulted from an Mpl-dependent processing of ActA between the AVC domain and the proline-rich region (Fig. 4B). To test our hypothesis, we generated a version of ActA-3xF lacking amino acid residues 207 to 238 (Fig. 4B, ActA-3xF-Δ207-238). Similar to the *mpl* mutant, the 30-kDa peptide was not observed in samples extracted from cells infected with the mutant strain expressing ActA-3xF-Δ207-238 (Fig. 4A), suggesting that amino acid residues 207 to 238 are required for Mpl-dependent processing of the N-terminal region of ActA. Interestingly, the abundances of high-molecular-weight species were similar for wild-type and mutant bacteria, indicating that the 30-kDa peptide results from ActA processing in a minor proportion of bacteria in agreement with the notion that processing occurs only for bacteria in protrusions. We also noted that, in the absence of N-terminal processing of ActA-3xF-Δ207-238, we detected high-molecular-weight species slightly shorter than full-length ActA, suggesting that ActA was also processed in the C-terminal region. These results support the notion that Mpl mediates ActA polarization in protrusions through the release of ActA from the bacterial side, a regulatory event that requires ActA amino acid residues 207 to 238.

Polarization of ActA-Δ207-238 in protrusions. We next compared the surface levels of ActA in the protrusions formed in cells infected with wild-type *actA-3xF* and *actA-3xF-Δ207-238* mutant strains. As conducted for the *mpl* mutant (Fig. 3), we determined the intensity of the Flag signal along the bacterial length for wild-type bacteria and the *actA-3xF-Δ207-238* mutant in protrusions. In contrast with the polarized distribution of the Flag signal in wild-type *actA-3xF* bacteria, *actA-3xF-Δ207-238* mutant displayed a striking increase in the levels of the Flag signal, with an abnormal distribution along the bacterial length (Fig. 5A and B; see also Fig. S4 in the supplemental

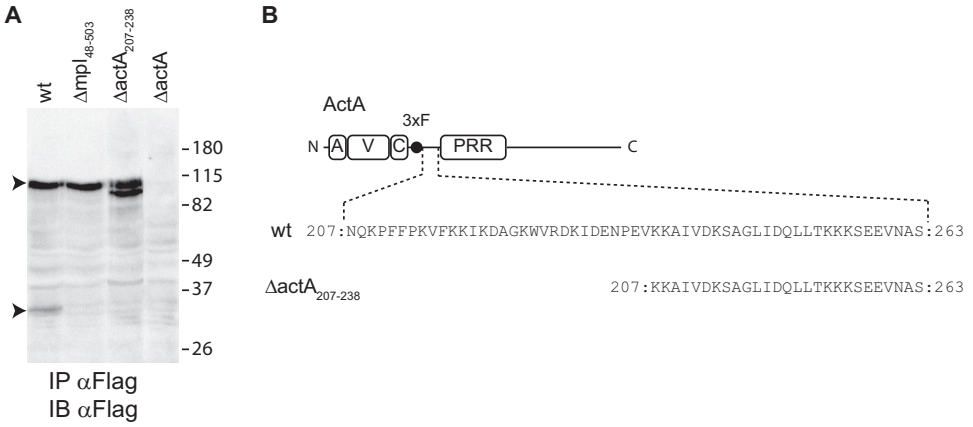

FIG 4 Mapping of an Mpl-dependent processing site in ActA. (A) Western blot of ActA 3×F immunoprecipitated (IP) from cell lysates infected with *L. monocytogenes* wild-type, Δ*mpl*$_{48–503}$, Δ*actA*$_{207–238}$, or Δ*actA* strains. Arrowheads indicate ActA peptides of 90 and 30 kDa. Apparent molecular weights (in thousands) in the protein ladder are indicated on the right. IB, immunoblot. (B) Schematic representation of 3×Flag-ActA and in-frame deletion of ActA residues 207 to 238. Numbers indicate the first and last residues.

material). These results show that the defect in ActA processing associated with deletion of amino acid residues 207 to 238 correlates with a dramatic increase in ActA surface levels in protrusions.

The Δ*actA*$_{207–238}$ mutant displays wild-type actin-based motility. We next addressed whether the observed processing defects of ActA-3xF-Δ207-238 may impact the efficiency of actin-based motility. To this end, we compared the cytosolic velocity of bacteria using live cell imaging of cells infected with wild-type bacteria or mutant strains. Measurements of the velocity of bacteria in the cytosol of cells infected with the Δ*actA*$_{207–238}$ mutant did not reveal any significant differences compared to the velocity recorded in the cytosol of cells infected with wild-type bacteria or the *mpl* mutant (see Fig. S2 in the supplemental material). These results indicate that a defect in ActA processing due to either deletion of *mpl* or deletion of the Mpl-dependent processing site in ActA does not affect actin-based motility in the cytosol of infected cells.

ActA processing is required for the formation of wild-type infection foci. We next tested whether similar to the situation observed with the *mpl* mutant, the defect in ActA processing due to deletion of amino acid residues 207 to 238 in ActA affected the efficiency of cell-to-cell spread. To this end, we used fluorescence microscopy to compare focus size in cells infected with wild-type *actA-3xF* and the *actA-3xF-*Δ*207-238* mutant strain expressing GFP. As observed for the *mpl* deletion mutant (Fig. 1A), the *actA-3xF-*Δ*207-238* mutant bacteria showed a 36% ($P < 0.0001$) decrease in the size of the formed foci compared to those of wild-type bacteria (Fig. 6A and B). These results show that the defect in ActA processing associated with deletion of amino acid residues 207 to 238 correlates with a defect in cell-to-cell spread.

ActA processing is required for efficient resolution of protrusions into vacuoles. We next determined whether the spreading defect observed with the Δ*actA*$_{207–238}$ mutant was related to a defect in the resolution of protrusions into vacuoles. Similar to the situation observed with the *mpl* mutant, cells infected with the *actA-3xF-*Δ*207-238* mutant displayed a significant increase in the number of protrusions (Fig. 7A and B). Interestingly, the significant increase in the numbers of vacuoles observed in cells infected with the *mpl* mutant (Fig. 2) was not observed in cells infected with the *actA-3xF-*Δ*207-238* mutant, suggesting that the Mpl-de-

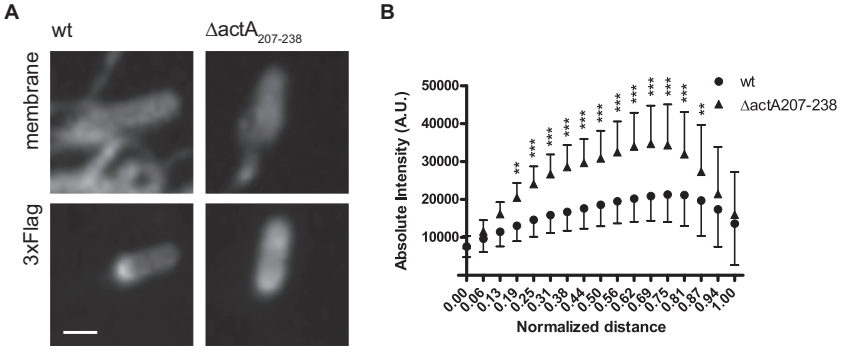

FIG 5 Distribution of ActA on the surface of wild-type and Δ*actA*$_{207–238}$ mutant bacteria forming protrusions. (A) Representative images showing the distribution of 3×Flag-ActA on the surface of bacteria in protrusions. Top panels, plasma membrane. Bottom panels, FLAG staining. Bar, 1 μm. (B) Quantification of ActA distribution on the bacterial surface. The absolute intensity of the FLAG signal is represented against the normalized distance from the front pole. Data are represented as means and standard deviations and were analyzed by two-way ANOVA using PRISM 5 (GraphPad Software). ***, $P < 0.001$; **, $P < 0.01$; *, $P < 0.05$.

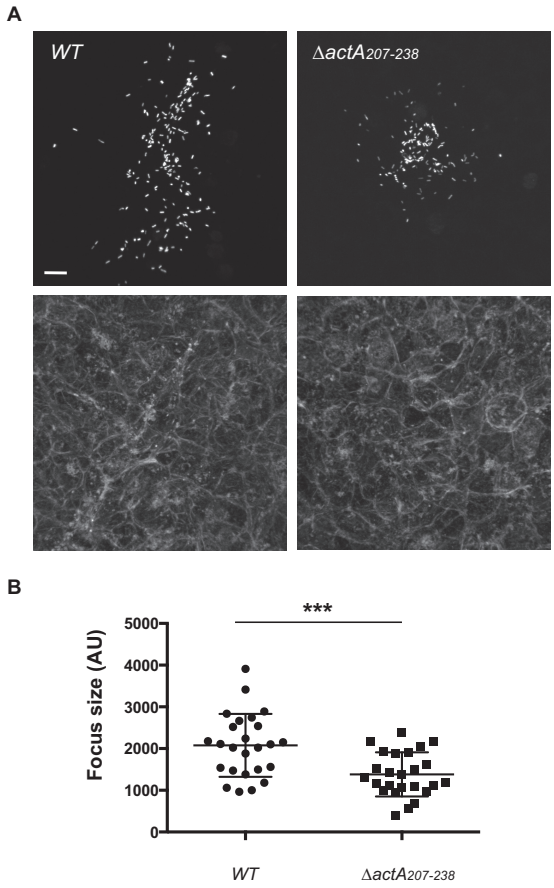

FIG 6 Characterization of the infection foci formed in cells infected with the wild-type or $\Delta actA_{207–238}$ mutant strains. (A) Representative images showing monolayers of confluent HeLa 229 cells infected with GFP-expressing *L. monocytogenes* for 6 h (top, GFP-expressing bacteria; bottom, phalloidin staining). Bar, 10 μm. (B) Sizes of the infection foci as determined by computer-assisted analysis of images like those shown in panel A. Unpaired *t* test: $\Delta actA_{207–238}$ versus WT strain, $P < 0.001$ (***).

pendent processing of ActA is not required for vacuole escape. Altogether, these results indicate that the Mpl-dependent processing of ActA contributes to the efficiency of protrusion resolution into vacuoles.

DISCUSSION

Genetic studies have established that *L. monocytogenes* dissemination relies on the *mlp-actA-plcB* operon (11), which encodes ActA, the bacterial factor responsible for actin-based motility (6), and PlcB, a phospholipase that mediates vacuole escape (33). As the metalloprotease Mpl was shown to activate the proenzyme PlcB required for vacuole escape (20), it was generally assumed that Mpl contributed to *L. monocytogenes* dissemination solely through vacuole escape. Here, using an assay allowing for the numeration of protrusions and vacuoles, we demonstrated that, unlike PlcB, Mpl is required for the efficient resolution of protrusions into vacuoles. We have previously shown that *L. monocytogenes* protrusion resolution relies on efficient actin polymerization at the bacterial pole (27), which presumably contributes the tension forces that challenge the plasma membrane and lead to vacuole formation. In the cytosol, efficient actin polymerization at the bacterial pole is supported by ActA polarization on the bacterial surface (15, 16, 35). ActA is secreted at distinct sites between the septation site and the old poles and then redistributed to the cylindrical bacterial body as a consequence of cell wall growth (15). It is assumed that differences in the dynamics of cell wall growth along dividing bacteria result in ActA polarization after several rounds of bacterial division (15). Bacteria rarely divide in protrusions, and how polarization is thus maintained in order to sustain efficient actin polymerization at the bacterial pole is unknown. Our results indicate that Mpl regulates the levels of ActA on the bacterial side in protrusions. We thus propose that Mpl supports protrusion resolution by maintaining ActA polarization in protrusions, thereby contributing to efficient actin polymerization at the bacterial pole. As the $\Delta actA_{207–238}$ deletion mutant phenocopies all the defects observed in cells infected with the *mpl* mutant, it is likely that the region encompassing amino acid residues 207 to 238 harbors an Mpl-dependent processing site, although our data do not exclude the possibility that Mpl may play an indirect role in the regulation of ActA processing. Further biochemical studies will be required to determine whether ActA may be a direct substrate of Mpl proteolytic activity.

In addition to the polarization of full-length ActA, the processing of ActA has two consequences that may be functionally important in the context of protrusion resolution. First, the release of the N-terminal (AVC) domain produces a truncated version of ActA encompassing the proline-rich region and the C terminus of the protein that remains anchored at the bacterial surface. Exposing the PRR of ActA on the bacterial side may generate docking sites for proline recognition modules such as Src homology 3 (SH3), WW (named for a conserved Trp-Trp motif), and Ena/VASP homology (EVH1 domains) (36), present in cellular factors potentially required for protrusion resolution. Second, ActA processing leads to the release of the N-terminal (AVC) domain, which may have a functional role in protrusion resolution. Interestingly, the A region of the AVC domain has been implicated in escape from the primary vacuole formed upon invasion, potentially through destabilization of the plasma membrane (37). It is thus tempting to speculate that the release of the AVC domain in protrusions may challenge the integrity of the plasma membrane, which in combination with the tension forces generated by actin polymerization at the bacterial pole may lead to protrusion resolution. We attempted to test this hypothesis by rescuing the protrusion resolution defect displayed by the *mpl* mutant by expressing a secreted version of the AVC domain of ActA. However, the expression of the corresponding constructs encoding the AVC domain only was toxic to bacteria, severely affecting bacterial growth for unknown reasons (data not shown). Although this observation may underscore the functional importance of the Mpl-mediated mechanism leading to the production of the AVC domain of ActA in a posttranscriptional manner, the potential contribution of the AVC domain to protrusion resolution remains to be explored.

Previous work uncovered the role of Mpl in the regulation of PlcB processing and vacuole escape (20, 25, 32). Our present work now establishes the role of Mpl in ActA processing and protrusion resolution. Numerous *L. monocytogenes* strains have been sequenced, and it is remarkable that the *mpl*, *actA*, and *plcB* genes are systematically organized as an operon (38). We

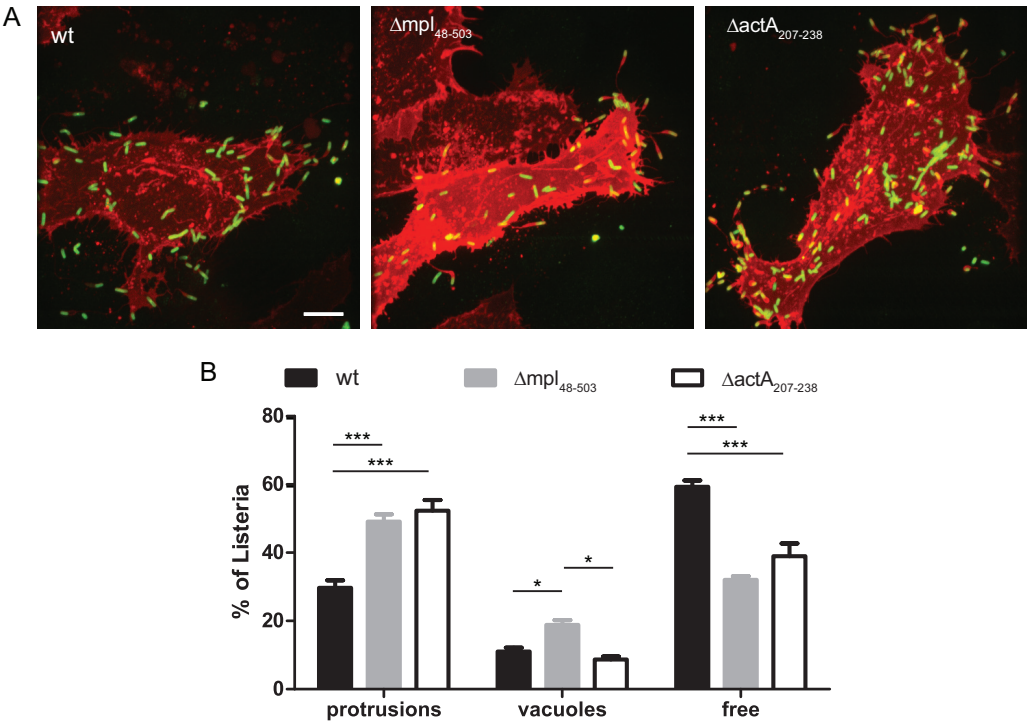

FIG 7 Protrusion resolution and vacuole escape in cells infected with the *mpl* and Δ*actA*$_{207–238}$ mutant strains. (A) Representative images showing protrusion and vacuole formation in HeLa 229 cells transiently transfected with the plasma membrane-targeted dsRed constructs and infected with GFP-expressing *L. monocytogenes* for 6 h (green, bacteria; red, membrane). Bar, 10 μm. (B) Percentages of spreading bacteria in protrusions, in vacuoles, and free in adjacent cells in cells infected with the wild-type bacteria or with *mpl* or Δ*actA*$_{207–238}$ mutant strains. Data are presented as means and standard deviations for three independent samples and were analyzed by two-way ANOVA with Tukey's posttest using PRISM 5 (GraphPad Software). ***, $P < 0.001$; *, $P < 0.05$.

suggest that this physical linkage reflects the functional importance of regulating the activities of ActA and PlcB through Mpl-dependent processing in the context of *L. monocytogenes* dissemination.

ACKNOWLEDGMENTS

We thank past and present members of the Agaisse laboratory for discussions and comments on the manuscript. The main body of this work was conducted at Yale University, in the Department of Microbial Pathogenesis. We thank Jorge Galan, Chair of the Department of Microbial Pathogenesis, for his continuous support.

FUNDING INFORMATION

This work, including the efforts of Herve Agaisse, was funded by HHS | NIH | NIAID (R01AI073904).

REFERENCES

1. **Gouin E, Welch MD, Cossart P.** 2005. Actin-based motility of intracellular pathogens. Curr Opin Microbiol **8:**35–45. http://dx.doi.org/10.1016/j.mib.2004.12.013.
2. **Robbins JR, Barth AI, Marquis H, de Hostos EL, Nelson WJ, Theriot JA.** 1999. *Listeria monocytogenes* exploits normal host cell processes to spread from cell to cell. J Cell Biol **146:**1333–1350. http://dx.doi.org/10.1083/jcb.146.6.1333.
3. **Tilney LG, Portnoy DA.** 1989. Actin filaments and the growth, movement, and spread of the intracellular bacterial parasite, *Listeria monocytogenes*. J Cell Biol **109:**1597–1608. http://dx.doi.org/10.1083/jcb.109.4.1597.
4. **Dragoi AM, Agaisse H.** 2015. The class II phosphatidylinositol 3-phosphate kinase PIK3C2A promotes *Shigella flexneri* dissemination through formation of vacuole-like protrusions. Infect Immun **83:**1695–1704. http://dx.doi.org/10.1128/IAI.03138-14.
5. **Kuehl CJ, Dragoi AM, Talman A, Agaisse H.** 2015. Bacterial spread from cell to cell: beyond actin-based motility. Trends Microbiol **23:**558–566. http://dx.doi.org/10.1016/j.tim.2015.04.010.
6. **Kocks C, Gouin E, Tabouret M, Berche P, Ohayon H, Cossart P.** 1992. *L. monocytogenes*-induced actin assembly requires the actA gene product, a surface protein. Cell **68:**521–531.
7. **Brundage RA, Smith GA, Camilli A, Theriot JA, Portnoy DA.** 1993. Expression and phosphorylation of the *Listeria monocytogenes* ActA protein in mammalian cells. Proc Natl Acad Sci U S A **90:**11890–11894. http://dx.doi.org/10.1073/pnas.90.24.11890.
8. **Domann E, Wehland J, Rohde M, Pistor S, Hartl M, Goebel W, Leimeister-Wachter M, Wuenscher M, Chakraborty T.** 1992. A novel bacterial virulence gene in *Listeria monocytogenes* required for host cell microfilament interaction with homology to the proline-rich region of vinculin. EMBO J **11:**1981–1990.
9. **Skoble J, Portnoy DA, Welch MD.** 2000. Three regions within ActA promote Arp2/3 complex-mediated actin nucleation and *Listeria monocytogenes* motility. J Cell Biol **150:**527–538. http://dx.doi.org/10.1083/jcb.150.3.527.
10. **Welch MD, Iwamatsu A, Mitchison TJ.** 1997. Actin polymerization is induced by Arp2/3 protein complex at the surface of *Listeria monocytogenes*. Nature **385:**265–269. http://dx.doi.org/10.1038/385265a0.
11. **Vazquez-Boland JA, Kocks C, Dramsi S, Ohayon H, Geoffroy C, Mengaud J, Cossart P.** 1992. Nucleotide sequence of the lecithinase operon of *Listeria monocytogenes* and possible role of lecithinase in cell-to-cell spread. Infect Immun **60:**219–230.
12. **Bohne J, Sokolovic Z, Goebel W.** 1994. Transcriptional regulation of prfA and PrfA-regulated virulence genes in *Listeria monocytogenes*. Mol Microbiol **11:**1141–1150. http://dx.doi.org/10.1111/j.1365-2958.1994.tb00390.x.
13. **Shetron-Rama LM, Marquis H, Bouwer HG, Freitag NE.** 2002. Intracellular induction of *Listeria monocytogenes* actA expression. Infect Immun **70:**1087–1096. http://dx.doi.org/10.1128/IAI.70.3.1087-1096.2002.
14. **Mengaud J, Dramsi S, Gouin E, Vazquez-Boland JA, Milon G, Cossart**

P. 1991. Pleiotropic control of *Listeria monocytogenes* virulence factors by a gene that is autoregulated. Mol Microbiol **5:**2273–2283. http://dx.doi.org/10.1111/j.1365-2958.1991.tb02158.x.
15. **Rafelski SM, Theriot JA.** 2006. Mechanism of polarization of *Listeria monocytogenes* surface protein ActA. Mol Microbiol **59:**1262–1279. http://dx.doi.org/10.1111/j.1365-2958.2006.05025.x.
16. **Smith GA, Portnoy DA, Theriot JA.** 1995. Asymmetric distribution of the *Listeria monocytogenes* ActA protein is required and sufficient to direct actin-based motility. Mol Microbiol **17:**945–951. http://dx.doi.org/10.1111/j.1365-2958.1995.mmi_17050945.x.
17. **Camilli A, Tilney LG, Portnoy DA.** 1993. Dual roles of plcA in *Listeria monocytogenes* pathogenesis. Mol Microbiol **8:**143–157. http://dx.doi.org/10.1111/j.1365-2958.1993.tb01211.x.
18. **Grundling A, Gonzalez MD, Higgins DE.** 2003. Requirement of the *Listeria monocytogenes* broad-range phospholipase PC-PLC during infection of human epithelial cells. J Bacteriol **185:**6295–6307. http://dx.doi.org/10.1128/JB.185.21.6295-6307.2003.
19. **Forster BM, Marquis H.** 2012. Protein transport across the cell wall of monoderm Gram-positive bacteria. Mol Microbiol **84:**405–413. http://dx.doi.org/10.1111/j.1365-2958.2012.08040.x.
20. **Marquis H, Hager EJ.** 2000. pH-regulated activation and release of a bacteria-associated phospholipase C during intracellular infection by *Listeria monocytogenes*. Mol Microbiol **35:**289–298. http://dx.doi.org/10.1046/j.1365-2958.2000.01708.x.
21. **Snyder A, Marquis H.** 2003. Restricted translocation across the cell wall regulates secretion of the broad-range phospholipase C of *Listeria monocytogenes*. J Bacteriol **185:**5953–5958. http://dx.doi.org/10.1128/JB.185.20.5953-5958.2003.
22. **O'Neil HS, Forster BM, Roberts KL, Chambers AJ, Bitar AP, Marquis H.** 2009. The propeptide of the metalloprotease of *Listeria monocytogenes* controls compartmentalization of the zymogen during intracellular infection. J Bacteriol **191:**3594–3603. http://dx.doi.org/10.1128/JB.01168-08.
23. **Bitar AP, Cao M, Marquis H.** 2008. The metalloprotease of *Listeria monocytogenes* is activated by intramolecular autocatalysis. J Bacteriol **190:**107–111. http://dx.doi.org/10.1128/JB.00852-07.
24. **Forster BM, Bitar AP, Slepkov ER, Kota KJ, Sondermann H, Marquis H.** 2011. The metalloprotease of *Listeria monocytogenes* is regulated by pH. J Bacteriol **193:**5090–5097. http://dx.doi.org/10.1128/JB.05134-11.
25. **Yeung PS, Zagorski N, Marquis H.** 2005. The metalloprotease of *Listeria monocytogenes* controls cell wall translocation of the broad-range phospholipase C. J Bacteriol **187:**2601–2608. http://dx.doi.org/10.1128/JB.187.8.2601-2608.2005.
26. **Chong R, Squires R, Swiss R, Agaisse H.** 2011. RNAi screen reveals host cell kinases specifically involved in *Listeria monocytogenes* spread from cell to cell. PLoS One **6:**e23399. http://dx.doi.org/10.1371/journal.pone.0023399.
27. **Talman AM, Chong R, Chia J, Svitkina T, Agaisse H.** 2014. Actin network disassembly powers dissemination of *Listeria monocytogenes*. J Cell Sci **127:**240–249. http://dx.doi.org/10.1242/jcs.140038.
28. **Bishop DK, Hinrichs DJ.** 1987. Adoptive transfer of immunity to *Listeria monocytogenes*. The influence of in vitro stimulation on lymphocyte subset requirements. J Immunol **139:**2005–2009.
29. **Arantes O, Lereclus D.** 1991. Construction of cloning vectors for *Bacillus thuringiensis*. Gene **108:**115–119. http://dx.doi.org/10.1016/0378-1119(91)90495-W.
30. **Arnaud M, Chastanet A, Debarbouille M.** 2004. New vector for efficient allelic replacement in naturally nontransformable, low-GC-content, gram-positive bacteria. Appl Environ Microbiol **70:**6887–6891. http://dx.doi.org/10.1128/AEM.70.11.6887-6891.2004.
31. **Sun AN, Camilli A, Portnoy DA.** 1990. Isolation of *Listeria monocytogenes* small-plaque mutants defective for intracellular growth and cell-to-cell spread. Infect Immun **58:**3770–3778.
32. **Marquis H, Goldfine H, Portnoy DA.** 1997. Proteolytic pathways of activation and degradation of a bacterial phospholipase C during intracellular infection by *Listeria monocytogenes*. J Cell Biol **137:**1381–1392. http://dx.doi.org/10.1083/jcb.137.6.1381.
33. **Smith GA, Marquis H, Jones S, Johnston NC, Portnoy DA, Goldfine H.** 1995. The two distinct phospholipases C of *Listeria monocytogenes* have overlapping roles in escape from a vacuole and cell-to-cell spread. Infect Immun **63:**4231–4237.
34. **Chong R, Swiss R, Briones G, Stone KL, Gulcicek EE, Agaisse H.** 2009. Regulatory mimicry in *Listeria monocytogenes* actin-based motility. Cell Host Microbe **6:**268–278. http://dx.doi.org/10.1016/j.chom.2009.08.006.
35. **Kocks C, Hellio R, Gounon P, Ohayon H, Cossart P.** 1993. Polarized distribution of *Listeria monocytogenes* surface protein ActA at the site of directional actin assembly. J Cell Sci **105**(Part 3):699–710.
36. **Holt MR, Koffer A.** 2001. Cell motility: proline-rich proteins promote protrusions. Trends Cell Biol **11:**38–46. http://dx.doi.org/10.1016/S0962-8924(00)01876-6.
37. **Poussin MA, Goldfine H.** 2010. Evidence for the involvement of ActA in maturation of the *Listeria monocytogenes* phagosome. Cell Res **20:**109–112. http://dx.doi.org/10.1038/cr.2009.142.
38. **Hain T, Steinweg C, Chakraborty T.** 2006. Comparative and functional genomics of *Listeria* spp. J Biotechnol **126:**37–51. http://dx.doi.org/10.1016/j.jbiotec.2006.03.047.